Electronic Supplementary Material (ESI) for Polymer Chemistry.

Supporting Information

Chitosan-based fluorescent hydrogel for selective detection of Fe^{2+} ions with gel-to-sol mode and turn-off fluorescent mode

Kaiqi Fan [a], Xiaobo Wang [b], Shuyan Yu [a], Guanglu Han [a], Die Xu [a], Liming Zhou*[a], Jian Song*[c]

Table of contents:

1. Experimental section

Synthesis of terpyridine-bearing aldehydes (P)

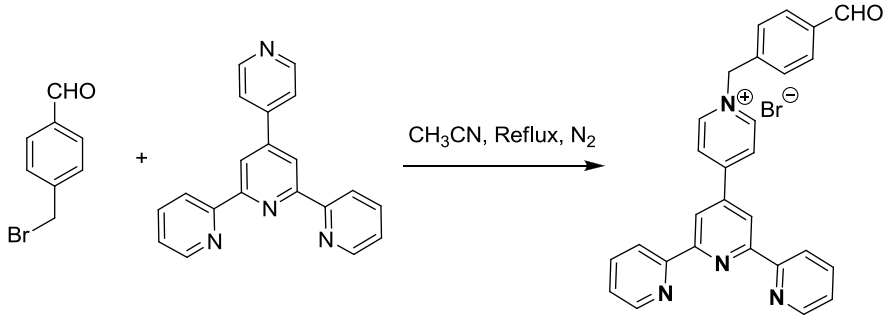

Scheme S1 Synthetic route to compound **P**.

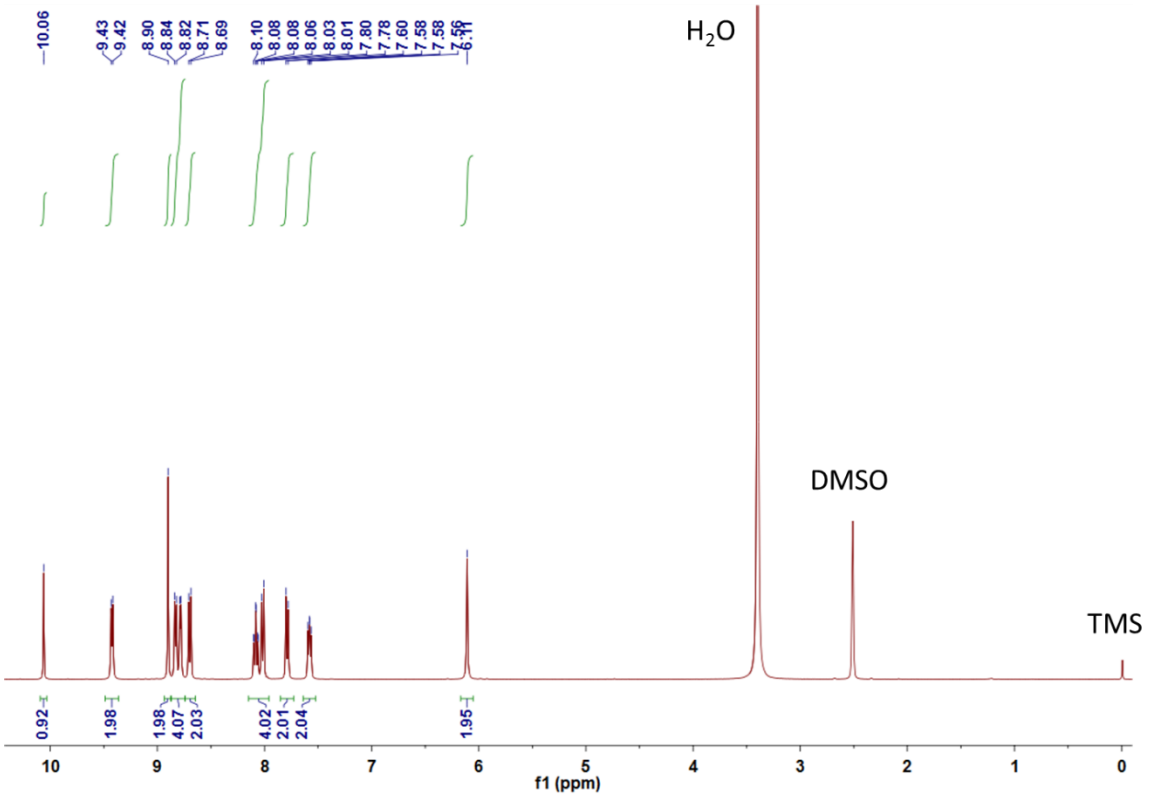

Fig. S1 ^{1}H NMR spectrum (400 MHz, DMSO-d6, 298 K) of compound P.

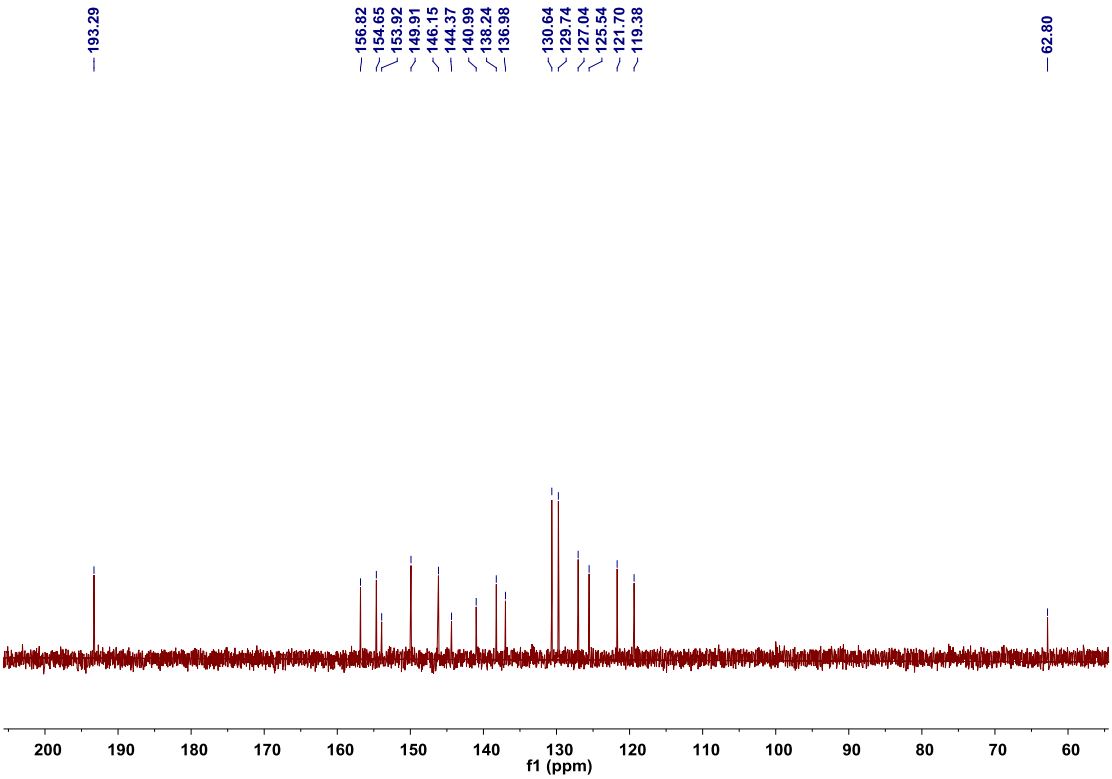

Fig. S2 ^{13}C NMR spectrum (400 MHz, DMSO-d6, 298 K) of compound P.

The gel-sol transition temperature (T_{gel}). The T_{gel} was determined by a conventional "ball-drop method". A small glass ball with a diameter of 5 mm (0.15 g) was placed on the top of the hydrogel in a test tube (10 mm diameter) which was in a thermostated oil bath and was heated at ca. 1.5 ℃/min. The temperature corresponding to submersion in the solution was regarded as the T_{gel} of the hydrogel. The measured experiments were carried out in duplicate.

The conversion rate (η%) of the aldehyde into imine units during the hydrogelation process. η% has been calculated with equation:

$$\eta\% = \frac{M_0 - M_r}{M_0} * 100$$

where M_0 is the amount of aldehyde used for hydrogel obtaining, and M_r represents the amount of aldehyde removed during the hydrogels washing, found as the difference between the initial amount of reagents (chitosan and aldehyde) and the amount of xerogel. This calculation supposed the total removal of the aldehyde during the washing and lyophilization processes.

Detection of metal ions by CP hydrogel. The salts of various metals, including chlorides of Fe^{2+}, Fe^{3+}, Cu^{2+}, Ni^{2+}, Mg^{2+} and Zn^{2+} were used for detection of metal ions in aqueous media. Stock solution (20×10^{-6} M) for different metal ions were prepared in distilled water (pH=7). Then, the metal solutions (50 μL each) were added to CP hydrogel (2 mL) at room temperature, and record the time required for the phase transition of gel-to-sol, as well as the time required for the color change.

Table S1 The time required for the phase transition of gel-to-sol and the color change

Metal ions	The time required for gel-to-sol	The time required for the color change
Fe^{2+}	10s	3s
Fe^{3+}	No change	No change
Cu^{2+}	No change	No change
Ni^{2+}	No change	No change
Mg^{2+}	No change	No change
Zn^{2+}	No change	No change

Preparation of the Polluted Samples: The preparation of the polluted sample 1 is to add the quantitative Fe^{2+} to a certain volume of tap water (normal sample 1). Similarly, the preparation of polluted sample 2 is to add Fe^{2+} to the river water (normal sample 2). The concentration of both samples is 20×10^{-6} M.

Selectivity studies: The selectivity of the CP1 hydrogel for Fe^{2+}-selective were further determined by the competition experiments in background of various competing metal ions. The UV and fluorescence spectra were investigated after the addition of Fe^{2+} and other metal ions (Mg^{2+}, Cu^{2+}, Ni^{2+}, Fe^{3+}, Zn^{2+}) in the same concentration.

Instrumentation

NMR experiments: ^{1}H-NMR spectra were recorded on a Bruker DPX 400 MHz spectrometer (Bruker, USA) with 16 scans in D_2O and DMSO-d_6. The chemical shifts were reported as δ values (ppm) relative to the residual peak of the solvent. The hydrogel sample has been prepared in the NMR tube using deuterated solvents (D_2O and a few drops of trifluoroacetic acid-d_1 to solve chitosan, DMSO-d_6 to solve the aldehyde).

Mass spectrometry: Mass spectra were recorded on a TOF-QII high-resolution mass spectrometer.

Scanning Electron Microscope (SEM): The morphologies of the xerogels were obtained by a Hitachi S-4800 (Hitachi, Japan) microscope operating at 3-5 kV. Firstly, small portions of the gels, produced at 25 ºC, were placed on a glass cover slip. They were dried in air at room temperature and finally in a vacuum for three days, and then placed on the thin aluminum sheets. Subsequently, before the experiment, we coated the sample with a thin layer of Au.

FT-IR spectroscopy: FTIR measurements were performed on a FTS3000 spectrometer (Digilab Company, USA) with KBr pellets. The absorption spectra of the xerogels were obtained at room temperature in the range of 500-4000 cm^{-1} and a resolution of 2 cm^{-1}.

UV spectroscopy: UV spectroscopy was performed on a Jasco V-570 UV/vis/NIR spectrophotometer (JASCO, Japan), by using very thin hydrogel films deposited on glass plates.

Fluorescence emission spectroscopy: Fluorescence emission spectra were recorded on a Hitachi F-2500 fluorimeter (Hitachi, Japan), by exciting the samples with a light of wavelength corresponding to the absorption maxima from the UV-vis spectra, at room temperature. To obtain a good optical luminescence signal-to-noise ratio, the slit widths and detector parameters were optimized to maximize but not saturate the excitation Rayleigh peak. The measurements were carried out in triplicate for each sample.

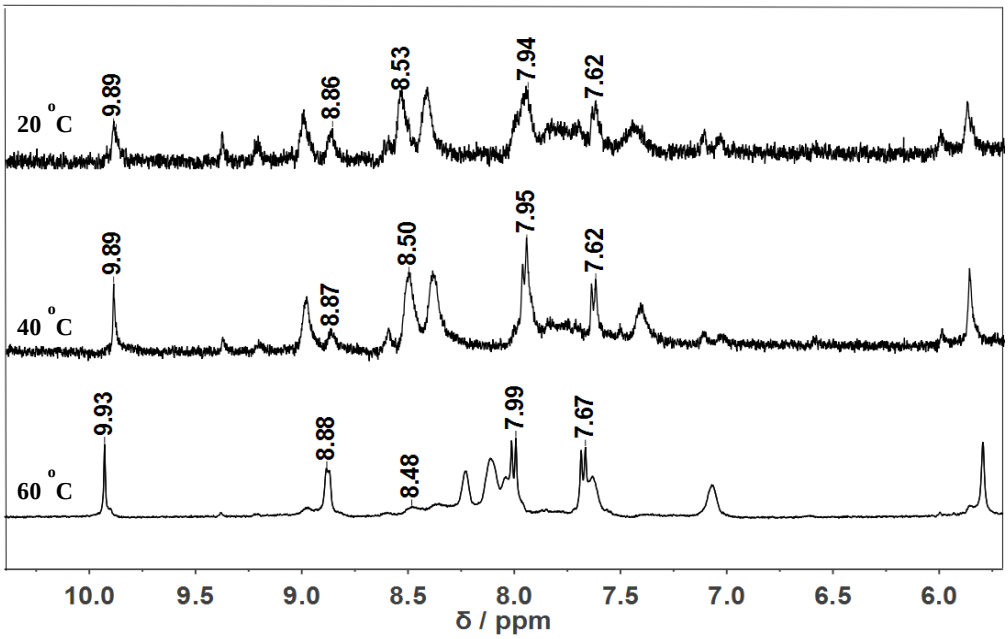

Fig. S3 ^{1}H-NMR spectra of CP1 hydrogel at different temperatures.

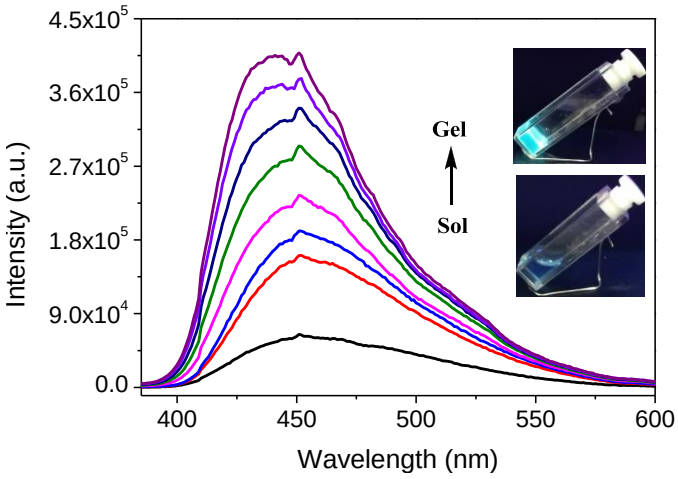

Fig. S4 Temperature-dependent fluorescence emission spectrum of CP1 hydrogel (λex = 365 nm). Inset: photographs of the sol and gel under irradiation with UV light at 365 nm.

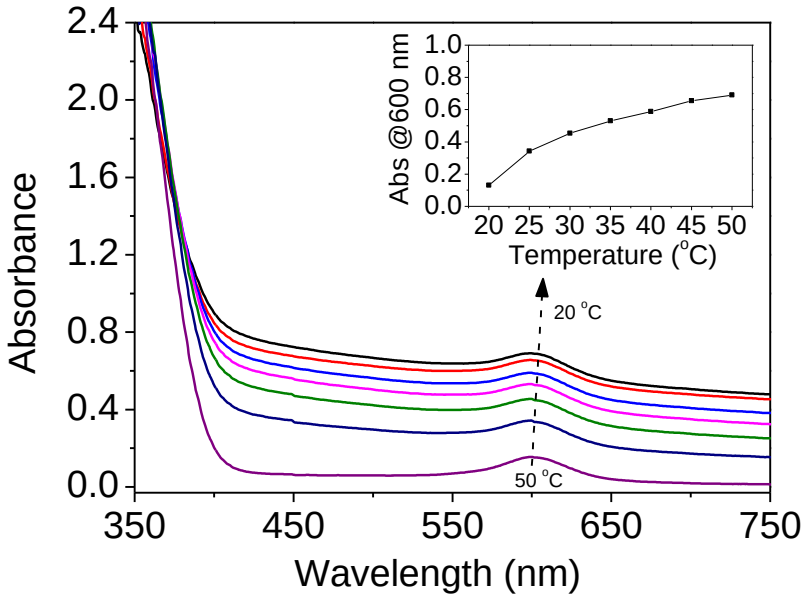

Fig. S5 Variable-temperature UV/vis absorption spectra of CP1 hydrogel. The arrows indicate spectral changes with decreasingtemperature. The inset shows a plot of absorption at 600nm against the temperature.

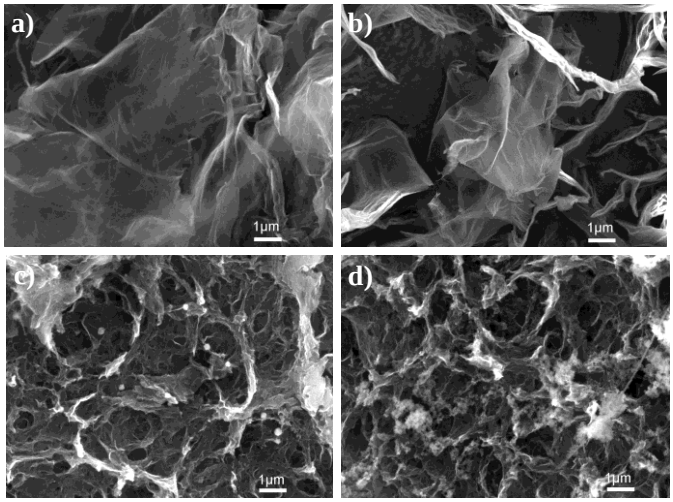

Fig. S6 SEM microphoto graphs of the xerogels of a) CP1; b) CP2; c) CP3; d) CP4.

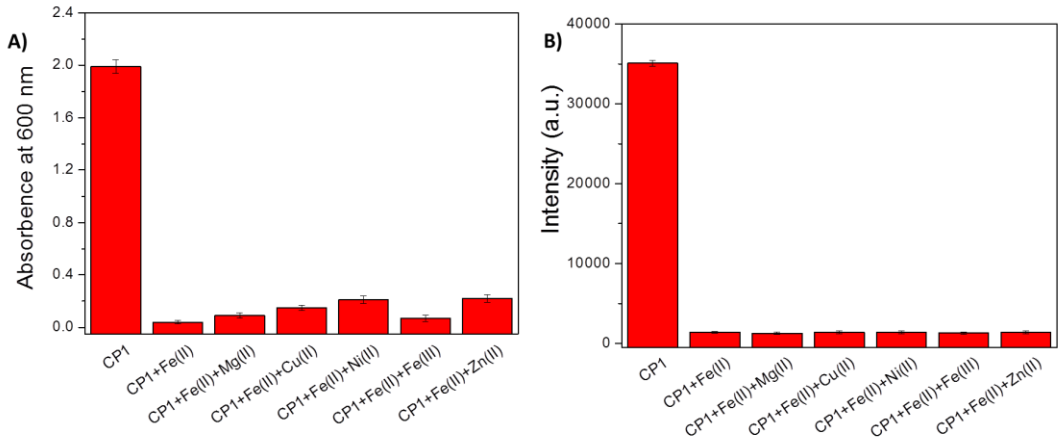

Fig. S7 Competitive selectivities of CP1 hydrogle (2 mL) toward Fe^{2+} in the presence of other metal ions (100 μL, 20×10^{-6} M).

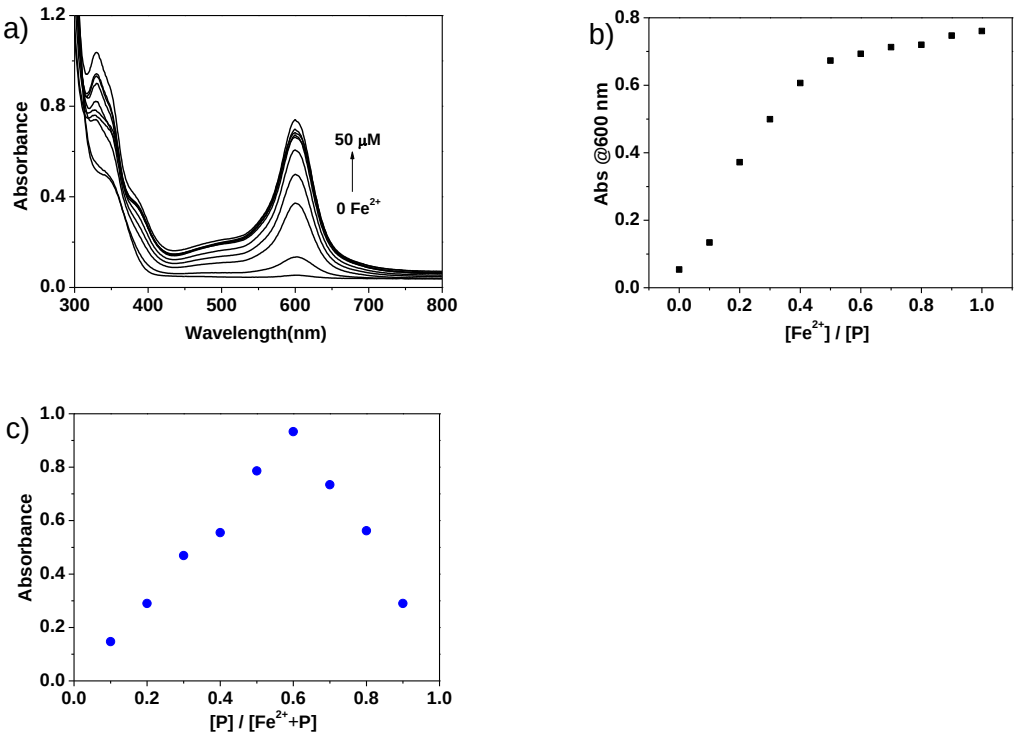

Fig. S8 (a) Absorption spectra of CP hydrogel in the presence of increasing concentration of Fe^{2+} ions. [P] Indicates the concentration of P in the CP1 hydrogel. (b) Plots of absorbance at 600 nm versus $[Fe^{2+}]$/ [P] derived from Fig. S7(a). (c) Job plot of CP and the Fe^{2+} ion complex.

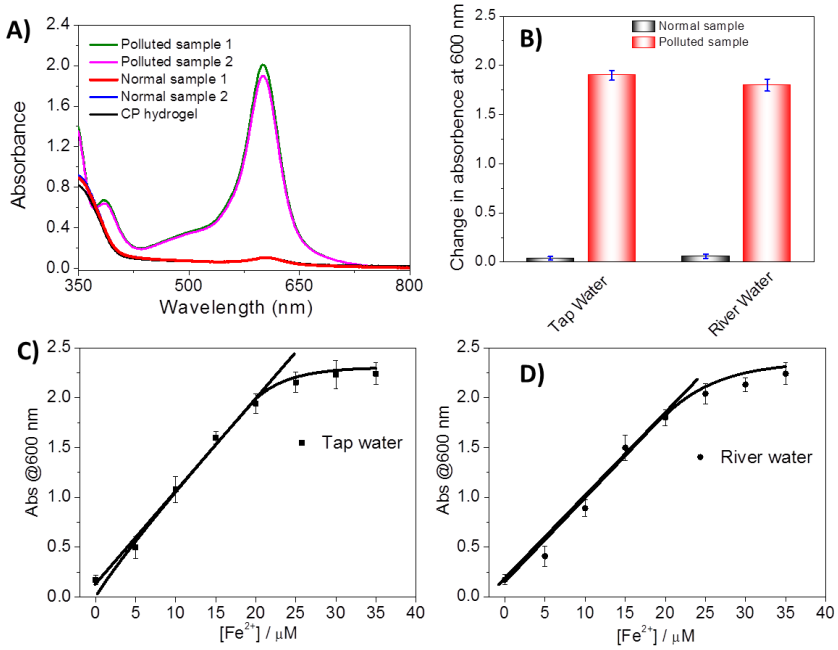

Fig. S9 (A) UV/vis absorption spectra and (B) the change in absorbance at 600 nm of the CP1 hydrogle in response to some normal and Fe^{2+}-polluted real-world water samples. Calibration curve for tap water (C) and river water (D). Error bars represent the standard deviations of triplicate experiments.

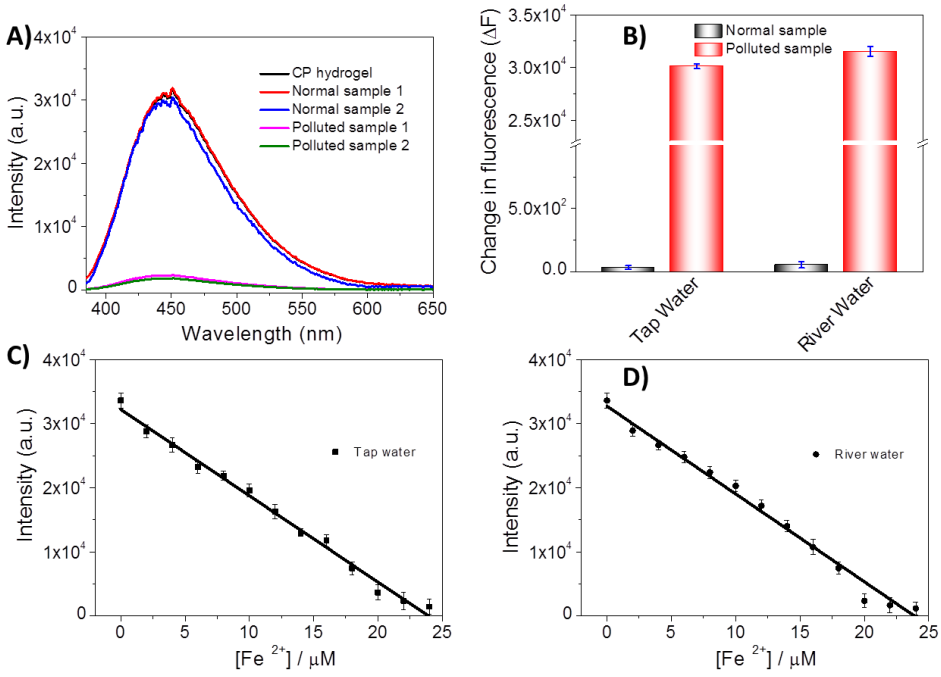

Fig. S10 (A) Fluorescence spectra and (B) the change in fluorensence (ΔF) of the CP1 hydrogle in response to some normal and Fe^{2+}-polluted real-world water samples. Calibration curve for tap water (C) and river water (D). Error bars represent the standard deviations of triplicate experiments.